HHS Public Access

Author manuscript

Cell Rep. Author manuscript; available in PMC 2019 January 24.

Published in final edited form as:

Cell Rep. 2018 December 11; 25(11): 2981–2991.e3. doi:10.1016/j.celrep.2018.11.017.

Regional Control of Hairless versus Hair-Bearing Skin by *Dkk2*

Yaolin Song[1,2], **Ana C. Boncompagni**[2], **Sang-Seok Kim**[2,3], **Heather R. Gochnauer**[2], **Yuhang Zhang**[4], **Gabriela G. Loots**[5,6], **Dianqing Wu**[7], **Yulin Li**[1], **Mingang Xu**[#2,*], and **Sarah E. Millar**[#2,8,9,11,*]

[1]The Key Laboratory of Pathobiology, Ministry of Education, Norman Bethune College of Medicine, Jilin University, Changchun, Jilin 130021, PRC

[2]Department of Dermatology, University of Pennsylvania Perelman School of Medicine, Philadelphia, PA 19104, USA

[3]Department of Dermatology, Hallym University Kangdong Sacred Heart Hospital, Seoul 134-701, Korea

[4]The James L. Winkle College of Pharmacy, University of Cincinnati, Cincinnati, OH 45267, USA

[5]School of Natural Sciences, University of California, Merced, CA 95343, USA

[6]Biology and Biotechnology Division, Lawrence Livermore National Laboratory, Livermore, CA 94550, USA

[7]Department of Pharmacology, Yale School of Medicine, New Haven, CT 06520, USA

[8]Department of Cell and Developmental Biology, University of Pennsylvania Perelman School of Medicine, Philadelphia, PA 19104, USA

[9]Department of Anatomy and Cell Biology, University of Pennsylvania School of Dental Medicine, Philadelphia, PA 19104, USA

[11]Lead Contact

[#] These authors contributed equally to this work.

SUMMARY

Haired skin is a defining characteristic of mammals. However, some specialized skin regions, such as human palms, soles and ventral wrist, and mouse plantar foot, are entirely hairless. Using mouse plantar skin as a model system, we show that the endogenous secreted Wnt inhibitor DKK2

[*]Correspondence: mingang@pennmedicine.upenn.edu (M.X.), millars@pennmedicine.upenn.edu (S.E.M.) https://doi.org/10.10167i.celrep.2018.11.017.

AUTHOR CONTRIBUTIONS

Y.S., A.C.B., S.-S.K., H.R.G., Y.Z., and M.X. conducted the experiments. Y.S., A.C.B., S.-S.K., H.R.G., Y.Z., M.X., and S.E.M. designed the experiments. D.W. generated and provided *Dkk2* mutant mice. G.G.L. provided *Sostdc1*^{lacZ} mice and helped design experiments. Y.L., M.X., and S.E.M. supervised the project. M.X. and S.E.M. conceived the project. Y.S., M.X., and S.E.M. wrote the paper.

DECLARATION OF INTERESTS

The authors declare no competing interests.

SUPPLEMENTAL INFORMATION

Supplemental Information includes three figures and one table and can be found with this article online at https://doi.org/10.1016/j.celrep.2018.11.017.

suppresses plantar hair follicle development and permits the formation of hairless skin. Plantar skin retains all of the mechanistic components needed for hair follicle development, as genetic deletion of *Dkk2* permits formation of fully functional plantar hair follicles that give rise to external hair, contain sebaceous glands and a stem cell compartment, and undergo regenerative growth. In the absence of *Dkk2,* Wnt/β-catenin signaling activity is initially broadly elevated in embryonic plantar skin and gradually becomes patterned, mimicking follicular development in normally haired areas. These data provide a paradigm in which regionally restricted expression of a Wnt inhibitor underlies specification of hairless versus hairy skin.

In Brief

What controls formation of hairless versus hairy skin? Song et al. find the secreted Wnt inhibitor *Dkk2* is specifically expressed in embryonic mouse hairless, but not in rabbit hair-bearing, plantar skin. Mouse *Dkk2* deletion permits plantar hair formation. Thus, evolutionary changes in *Dkk2* expression contribute to species-specific hair patterns.

Graphical Abstract

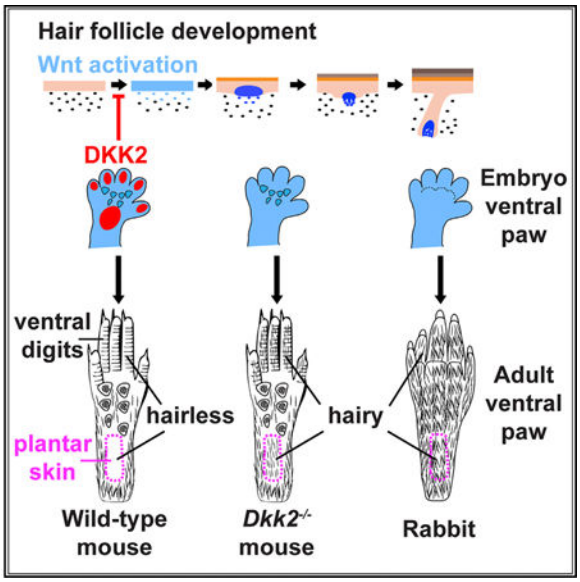

INTRODUCTION

While most body regions in mammals are covered in hair or fur of varying density, length, and thickness, certain areas remain completely hairless. Striking examples of this in humans are the palms of the hands, the ventral wrist, and the soles of the feet. In laboratory mice, a tractable model system for investigating the genetics underlying hair follicle development and patterning, plantar epidermis, analogous to human ventral wrist, and the eccrine sweat gland-bearing footpads, are hairless. By contrast, the skin in between the footpads displays a mixture of hair follicles and eccrine sweat glands whose relative numbers vary among mouse strains (Kamberov et al., 2015). Interestingly, plantar epidermis in rabbits and polar bears is furred, suggesting evolutionary adaptation of the mechanisms that regulate

formation of hairless versus hair-bearing skin. In humans, hairy cutaneous malformations of the palms and soles (OMIM: 139650) are extremely rare, but have been reported in two families as autosomal dominant traits (Jackson et al., 1975;Schnitzler, 1973) and in two additional unrelated cases (Mehregan and Cos-key, 1972).

Wnt/β-catenin signaling plays key roles in the initiation, spacing, and postnatal growth of hair follicles. Interaction of Wnt ligands with Frizzled receptors and LRP5/6 co-receptors inactivates a complex of proteins that otherwise degrades cyto plasmic β-catenin, allowing it to accumulate and translocate to the nucleus where it complexes with members of the LEF/TCF family of DNA binding factors to activate transcription of target genes (Clevers and Nusse, 2012). Activation of Wnt/β-catenin signaling in the upper dermis in response to epithelial Wnt ligands precedes hair follicle placode formation and is required for this process (Chen et al., 2012). Additionally, Wnt/β-catenin signaling within surface ectodermal cells is necessary for their adoption of hair follicle fate (Andl et al., 2002; Huelsken et al., 2001) Conversely, mutation of epithelial β-catenin to a constitutively active form causes premature and ectopic formation of hair follicle placodes (Närhi et al., 2008; Zhang et al., 2008). Mature hair follicle structures fail to form in embryonic epidermis expressing activated β-catenin (Närhi et al., 2008; Zhang et al., 2008), indicating that Wnt/β-catenin signaling must be tightly controlled for normal hair follicle development to occur.

Several families of endogenous secreted inhibitors function to limit activity of the Wnt/β-catenin signaling pathway. These include members of the Dickkopf (DKK) family of secreted proteins, which antagonize Wnt/β-catenin signaling by associating with the extracellular domain of Wnt co-receptors LRP5/6 (Bafico et al., 2001; Semënov et al., 2001) and the transmembrane proteins Kremen1/2 (Niehrs, 2006). The DKK/LRP/KRM complex is internalized, removing LRP from the cell surface and preventing Wnt ligands from activating β-catenin signaling (Niehrs, 2006). An unrelated Wnt inhibitor, SOSTDC1, similarly functions by binding the LRP extracellular domain (Lintern et al., 2009). SOSTDC1 acts to limit the size of primary hair follicle placodes and prevents hair follicle formation in specialized nipple skin (Ahn et al., 2010; Närhi et al., 2012) but is not reported to suppress hair follicle development in larger hairless regions such as plantar skin (Närhi et al., 2012).

Deletion of the *Dkk2* gene results in partial transformation of the cornea to a stratified epithelium that develops hair follicles (Mukhopadhyay et al., 2006). Forced expression of high levels of *Dkk2* after primary hair follicle induction completely suppresses the formation of secondary hair follicle placodes and causes decreased primary hair follicle placode density and loss of the normal regular spacing of placode formation (Sick et al., 2006), suggesting a possible role for WNT/DKK mutual antagonism in setting up the pattern of hair follicle placode spacing in hairy skin (Sick et al., 2006). However, definitive loss of function experiments supporting a requirement for *Dkk2* in placode induction or spacing have not been described.

To address this question, we analyzed skin phenotypes in *Dkk2* null mice. These analyses revealed that patterning and development of hair follicles in hairy skin was unaffected by loss of *Dkk2.* Remarkably, however, normally hairless plantar skin displayed fully formed,

mature hair follicles that gave rise to external hair, were associated with sebaceous glands, contained a stem cell compartment, and were capable of regenerative growth after hair plucking. In line with this striking observation, we found that while *Dkk2* is expressed at low levels in hairy skin of wild-type mouse embryos and neonates, high levels of *Dkk2* transcript localize specifically to plantar dermis. In the absence *Dkk2,* Wnt reporter gene expression is increased in embryonic plantar dermis and epidermis and subsequently becomes patterned, mimicking the gradual restriction of Wnt/β-catenin signaling that occurs during normal development of hair-bearing skin. Interestingly, we found that *Dkk2* levels are not elevated in plantar versus dorsal paw skin in rabbit embryos, which develop hair follicles in their plantar region. These data identify *Dkk2* as a Wnt inhibitor that is differentially expressed in mouse plantar versus hairy skin dermis and controls regional development of hairless skin. Our results further suggest that altered specification of hairless versus hairy skin in different mammalian species may be partially controlled by evolutionary changes in the regulation of *Dkk2* expression.

RESULTS

Dkk2 Null Mice Have Normally Spaced Hair Follicles but Develop Ectopic Plantar Hair

To determine the requirements for *Dkk2* in hair follicle development and patterning, we analyzed mice carrying a null mutation in *Dkk2* (Li et al., 2005). In adult $Dkk2^{-/-}$ mutant mice, the appearance of the hair coat was similar to that of wild-type litter-mate controls (Figure 1A). Histological analysis of dorsal skin revealed no differences in hair follicle development, orientation, or density between mutants and controls at postnatal day (P) 17 (Figures 1B and 1C). To determine whether such differences might be apparent at an earlier developmental stage, we imaged whole mounted dissected dorsal skin at P2. This revealed patterns and densities of primary and secondary hair follicles that were indistinguishable between $Dkk2^{-/-}$ and control skin (Figures 1D and1E). In line with this, the sizes and spacing of primary hair follicle placodes, marked by whole mount *in situ* hybridization for *Ctnnbl* (β-catenin) mRNA at embryonic day (E) 14.5, were similar in mutant and control embryos (Figures 1F and1G).

By contrast with the lack of abnormalities in hairy skin, $Dkk2^{-/-}$ mutants developed a striking phenotype of ectopic hair growth in normally hairless plantar skin (Figures 1H and1J). This phenotype was present in all of >40 adult *Dkk2* null mice observed grossly and in no wild-type $Dkk2^{+/+}$ or heterozygous $Dkk2^{+/-}$control littermates. The presence of external plantar hair was associated with hair follicle dermal papillae, revealed by staining for alkaline phosphatase, in $Dkk2^{-/-}$ mutant but not control plantar skin (Figures 1K and 1L). Closer inspection of the plantar region by scanning electron microscopy revealed that ectopic plantar hair in $Dkk2^{-/-}$ mutants extended as far as the most proximal footpad (Figures 1M-1P). We compared the morphology of plucked ectopic plantar hair with that of hair plucked from hairy regions of the ventral limb by light microscopy. Normal mouse hair falls into four classes: large guard over-hairs; shorter, straight awl hairs; auchene hairs that display one bend; and zigzag hairs that show several kinks. By contrast, ectopic mutant hair was straight and much shorter and finer than normal hair (Figure 1Q). Despite its small size, ectopic plantar hair re-grew following depilation at P60 (Figure 1R).

As the mutant and control mice were maintained on a mixed strain background, and hair growth varies among different mouse strains in inter-footpad regions of the ventral paw (Kamberov et al., 2015), we checked whether lack of plantar hair shows strain variability. We found that wild-type inbred C57BL/6, FVB/N, or CD-1 mice all lacked plantar hair (Figure S1). Thus, ectopic formation of plantar hair is specifically associated with *Dkk2* deletion.

Dkk2 Is Specifically Upregulated In Plantar Dermis of Mouse but Not Rabbit Embryos

Given the lack of phenotypes in hairy skin and the striking formation of ectopic hair in plantar skin of $Dkk2^{-/-}$ mice, we examined expression of *Dkk2* during mouse hairy and plantar skin development. Whole mount *in situ* hybridization of wild-type embryos at E14.5, when primary hair follicle placodes develop, showed intense expression of *Dkk2* in the developing cornea and in limb digits and low expression in the inter-placode regions of hairy skin (Figure 2A). *In situ* hybridization of sectioned wild-type dorsal skin at P0 similarly revealed absence of signal in hair follicles, and low levels of expression in the upper (papillary) dermis in inter-follicular skin (Figures 2B and 2C). By contrast with low level expression in hair-bearing embryonic and neonatal skin, whole mount *in situ* hybridization showed striking and specific expression of *Dkk2* in the plantar region of ventral hind paws at E15.5 (Figures 2D and 2E). Cryosectioning of whole mounted hind paws revealed specific, high level expression in plantar papillary dermis compared with low or undetectable levels in the adjacent footpad and in dorsal limb dermis (Figures 2F-2H). *Dkk2* transcripts were also detected in ventral but not dorsal dermis in limb digits, as well as in developing joint regions and nail epithelium (Figure 2I). In line with expression of *Dkk2* in wild-type ventral digit dermis, ventral digit skin is hairless in control mice and formed ectopic hairs in $Dkk2^{-/-}$ mutants (Figures S2A and S2B). $Dkk2^{-/-}$ mutants did not display obvious defects in nail growth, suggesting that *Dkk2* may act redundantly with other Wnt inhibitors in the nail.

Consistent with the pattern of *Dkk2* expression identified by *in situ* hybridization, quantitation of *Dkk2* mRNA levels revealed significantly elevated expression in wild-type plantar skin compared with dorsal paw skin at E18.5. By contrast, transcripts for the related Wnt inhibitors *Dkk1* and *Dkk4,* which are specifically expressed in hair follicles (Andl et al., 2002; Bazzi et al., 2007), were more abundant in dorsal paw skin than in plantar skin at this stage, and *Dkk3* and *Sostdc1* showed no significant differences in their levels in dorsal paw versus plantar skin (Figure 2J).

Quantitation of *Dkk2* mRNA levels in neonatal $Dkk2^{+/-}$ control heterozygous and $Dkk2^{-/-}$ homozygous mutant plantar skin showed that *Dkk2* levels were essentially undetectable in homozygous mutant plantar skin (Figure 2K). In line with this, whole mount *in situ* hybridization for *Dkk2* revealed lack of a specific signal in limb digits or plantar skin of $Dkk2^{-/-}$ embryos (Figures S2C-S2F).

Unlike in mice and humans, plantar skin in rabbits is hair bearing. Developing hair follicle structures were visible in both dorsal and plantar regions of whole mounted rabbit paw at E29 (roughly equivalent to E18.5 of mouse embryogenesis) (Figures 2Land 2M) and by histological analysis (Figures 2N-2P). Interestingly, qPCR revealed no significant differences in the abundance of *rDkk2* mRNA between rabbit plantar and dorsal paw skin at

E29 (Figure 2Q). Thus, lack of specific upregulation of *Dkk2* may permit the development of haired plantar skin in rabbits.

Formation of Ectopic Plantar Follicles Initiates in Late Embryogenesis

The first morphological sign of hair follicle development is the formation of a localized thickening of the epidermis, known as a placode. Placodal cells invaginate into the dermis and subsequently proliferate, forming a hair germ, which then elongates into the dermis. In parallel, signals from the placode induce condensation of underlying dermal cells, which eventually become the hair follicle dermal papilla and are almost completely enveloped by hair follicle epithelial cells in late embryogenesis and during the subsequent anagen growth phase (Millar, 2002). To determine the timing of ectopic hair follicle development, we analyzed plantar skin histology in $Dkk2^{+/+}$ or $Dkk2^{+/-}$ control littermate and $Dkk2^{-/-}$ mutant mice between E16.5 and P15. Placode structures were first apparent in mutant, but not control, plantar epidermis at E18.5 and hair germ structures with adjacent dermal condensates formed by P1 (Figures 3A-3F′; arrows in 3D′and 3F′). Postnatally, these structures continued to develop, forming associated sebaceous glands and keratinized hair shafts (Figures 3G–3J′; arrows in 3H′and 3J′). Stratification of plantar epidermis was unperturbed by loss of *Dkk2,* indicated by similar expression of the stratification markers KRT14, KRT10, involucrin, and loricrin in control and $Dkk2^{-/-}$ mutant plantar epidermis at P7 (Figures S3A-S3H‘). Immunofluorescence for the proliferation marker Ki67 revealed similar levels of proliferation in plantar epidermal basal cells of $Dkk2^{-/-}$ mutants and $Dkk2^{+/+}$ littermate controls, as well as the presence of proliferating cells in ectopic follicular structures in the mutants (Figures S3I-S3J′).

To definitively identify ectopic structures in $Dkk2^{-/-}$ mutant plantar skin as hair follicles, we used immunofluorescence for the transcription factor LHX2, which is expressed in hair follicles but not in sweat glands (Lu et al., 2016). As expected, LHX2 expression was detected in dorsal paw hair follicles in control littermate and mutant $Dkk2^{-/-}$ mice at E18.5, P1, and P7 (Figures 4A, 4B, 4E, 4F, 4I, and 4J). In plantar skin, specific signal for LHX2 was absent in controls at all stages analyzed; however ectopic structures in $Dkk2^{-/-}$ mutant plantar skin expressed LHX2 from P1, identifying these as hair follicles (Figures 4A, 4B, 4E, 4F, 4I, and 4J; yellow arrows). Upregulated expression of SOX9, a transcription factor essential for formation of the hair follicle outer root sheath and bulge stem cell compartment (Vidal et al., 2005), was detected in dorsal paw hair follicles in control littermate and mutant $Dkk2^{-/-}$ mice at E18.5 and P1 and in ectopic hair follicles in $Dkk2^{-/-}$ plantar skin (Figures 4C, 4D, 4G, and 4H, yellow arrows). Consistent with the production of external hair shafts by ectopic plantar follicles in $Dkk2^{-/-}$ mutants (Figures 1I-1R) and histological detection of hair shaft structures (Figures 3H′and 3J′), immunofluorescence with antibody AE13, which binds hair shaft keratins, was observed in ectopic plantar hair follicles at P7 (Figure 4J, white arrow), as well as in dorsal paw hair follicles of $Dkk2^{+/+}$ control and $Dkk2^{-/-}$ mutant mice, but was absent in control plantar skin (Figures 4I and4J). Hair follicle epithelial stem cells can be identified by the marker KRT15 (Morris et al., 2004). Immunofluorescence for KRT15 at P15 revealed its expression in ectopic plantar hair follicles in $Dkk2^{-/-}$ mutants (Figure 4L, yellow arrow), while KRT15 signal was absent in littermate control plantar skin (Figure 4K). Together with our observation that ectopic plantar hair was capable of

regeneration following depilation at P60 (Figure 1R), these results indicate that the ectopic hair follicles contained a functional stem cell compartment.

Dkk2 Suppresses Wnt/β-Catenin Signaling In Plantar Skin

Wnt/β-catenin signaling is required in both dermal and epithelial cells for embryonic hair follicle placode formation and promotes this process when forcibly activated (Andl et al., 2002; Huelsken et al., 2001; Närhi et al., 2008; Zhang et al., 2008; Chen et al., 2012). As *Dkk2* can function as a Wnt inhibitor, we asked whether Wnt/β-catenin signaling is enhanced in plantar skin of $Dkk2^{-/-}$ mice. *Dkk2* mutants were crossed to $Axin2^{lacZ}$ Wnt reporter mice, in which the *lacZ* gene is inserted into the *Axin2* locus, a ubiquitous target of Wnt/β-catenin signaling (Lustig et al., 2002). Whole mount staining for β-galactosidase at E17.5, 1 day before the morphological appearance of ectopic placodes in the mutants, revealed patches of highly increased Wnt reporter expression in the plantar region of whole mounted $Dkk2^{-/-}$ $Axin2^{lacZ}$ homozygous mutant hind paws compared with $Dkk2^{+/-}$ $Axin2^{lacZ}$ littermate controls (Figures 5A and 5B, arrows). Cryosectioning of ventral hind paw skin showed that Wnt reporter expression localized to footpad structures in both $Dkk2^{-/-}$ $Axin2^{lacZ}$ mutants and $Dkk2^{+/-}$ $Axin2^{lacZ}$ controls (Figures 5C and 5D, red arrows), but was strongly elevated in the dermis and epidermis of mutant plantar skin compared with control plantar skin (Figures 5C and 5D, yellow arrows). These data indicate that, in wild-type mouse embryos, DKK2 secreted from upper dermal cells inhibits Wnt/β-catenin signaling both in the papillary dermis and in adjacent epidermal cells.

LEF1 is a β-catenin transcriptional partner that is positively regulated by Wnt signaling and localizes to developing hair follicles (Huber et al., 1996; Liu et al., 2004; Zhou et al., 1995). Immunofluorescence staining revealed broadly enhanced LEF1 expression in $Dkk2^{-/-}$ compared with $Dkk2^{+/-}$ control plantar epidermis from as early as E16.5 (Figures 5E-5F', arrows). By P1, strong signal for LEF1 localized to ectopic hair germ structures (Figures 5G-5H′, arrows). As shown in Figures 5I-5J′, nuclear β-catenin localized to ectopic hair germ epithelium (yellow and green arrows in Figure 5J′) and dermal condensates (white arrow in Figure 5J′) in $Dkk2^{-/-}$ plantar skin at P1 but did not show specific upregulation in control plantar skin. Taken together, these data indicate that endogenous DKK2 functions to suppress Wnt/β-catenin signaling in plantar dermis and epidermis and allow the formation of hairless skin (Figures 5I and5I′).

The initial broad but patchy pattern of upregulation of Wnt/ β-catenin signaling in $Dkk2^{-/-}$ plantar skin and the small size of ectopic hairs could result from non-uniform expression of Wnt ligands and/or from the activity of additional Wnt inhibitors in the plantar region. In line with the latter hypothesis, we found that, while it is not differentially regulated in plantar versus dorsal paw skin (Figure 2J), expression of the secreted Wnt inhibitor *Sostdc1,* indicated by X-gal staining for a $Sostdc1^{lacZ}$ reporter allele (Yanagita et al., 2006), localized to basal plantar epidermis in $Sostdc1^{lacZ}$ control and $Sostdc1^{lacZ}Dkk2^{-/-}$ mutant mice and to ectopic hair follicles in the $Sostdc1^{lacZ}$ $Dkk2^{-/-}$ mutants (Figures 5K and 5L). *Sostdc1* could thus potentially act to limit Wnt signaling in the absence of *Dkk2.*

DISCUSSION

Wnt/β-catenin signaling plays key roles in initiating hair follicle development during embryogenesis (Andl et al., 2002; Huelsken et al., 2001; Chen et al., 2012). However, uncontrolled activity of the Wnt/β-catenin pathway prevents the morphogenesis of normally functioning, regularly spaced hair follicles (Närhi et al., 2008; Zhang et al., 2008). These observations suggest that endogenous Wnt inhibitory factors must control Wnt activity to permit normal patterning and development of hair follicles. Here, we investigated the functions of the secreted Wnt inhibitor DKK2 in these processes. Our analyses revealed a key and unexpected role for DKK2 in specifying hairless versus hairy skin.

While hair follicles developed normally in dorsal skin of mice lacking *Dkk2,* these mutants displayed a highly unusual phenotype of hair growth in the normally hairless plantar region of the mouse paw. Hair growth in this region was not observed in wild-type or heterozygous mutant littermate mice, or in wild-type mice of several common inbred strains. *In situ* hybridization and qPCR studies revealed that *Dkk2* is expressed at higher levels in plantar than in adjacent footpad skin or haired dorsal paw skin and localizes to the upper (papillary) dermis. Consistent with DKK2's function as a Wnt inhibitor in most *in vivo* contexts (Gage et al., 2008; Li et al., 2005; Li et al., 2012; Mukhopadhyay et al., 2006), Wnt signaling was elevated in plantar skin of $Dkk2^{-/-}$ mutant embryos, and this correlated with formation of ectopic hair follicle placodes in late embryogenesis. Although ectopic plantar hair was shorter and finer than any of the normal hair types in dorsal skin, the ectopic hair follicles expressed the stem cell marker KRT15 and regenerated external hair following depilation, indicating that they were fully functional and contained a stem cell compartment. Thus, *Dkk2* functions non-redundantly to suppress Wnt signaling and permit hair follicle development in the plantar region. This finding provides a paradigm to explain the formation of regions of hairless versus hairy skin.

In line with the restriction of high levels of endogenous *Dkk2* expression to the plantar region of ventral foot skin, formation of ectopic hair follicles in $Dkk2^{-/-}$ mice did not extend to the footpads, which are characterized by development of sweat glands but not hair follicles. Thus, the $Dkk2^{-/-}$ phenotype is distinct from that caused by mutation of epithelial β-catenin to a constitutively active form, which results in ectopic formation of hair follicles in the footpads and other normally hairless regions of ventral paw skin (Zhang et al., 2008). Forced expression of the BMP inhibitor Noggin also promotes hair follicle development in the footpads and suppresses sweat gland formation (Lu et al., 2016; Plikus and Chuong, 2004). Wnt/β-catenin signaling is normally elevated in footpad compared with dorsal skin dermis but is reduced in developing sweat gland compared with hair follicle epithelial cells (Lu et al., 2016). These effects correlate with elevated mesenchymal BMP signaling in footpad skin (Lu et al., 2016), but the underlying mechanisms connecting these two pathways in sweat gland development have not been fully delineated. The Wnt inhibitor *Dkk4* localizes to developing sweat gland buds and suppresses sweat gland formation when overexpressed (Cui et al., 2014); however, its requirement for sweat gland development has not been determined through genetic loss of function assays. Thus, the interesting question of the roles of secreted Wnt inhibitors in suppressing hair follicle development in the footpad, and in determining hair follicle versus sweat gland fate, has yet to be elucidated.

Despite its ability to alter hair follicle placode patterning in hairy skin when overexpressed (Sick et al., 2006), loss of endogenous *Dkk2* did not affect this process or other aspects of embryonic hair follicle development in hairy skin. *Dkk2* displays general, low level expression in embryonic and neonatal hairy skin dermis and is excluded from hair follicles at these stages. Its expression partially overlaps with that of transcripts for the related gene *Dkk1,* which localize to dermal cells adjacent to hair follicle placodes and germs (Andl et al., 2002; Narhi et al., 2008) and contrasts with that of *Dkk4,* a direct Wnt/β-catenin target that is specifically induced in placodes (Bazzi et al., 2007). Expression of the unrelated secreted Wnt inhibitor *Sostdc1* is excluded from hair follicle placodes at E14.5, but localizes to epidermal rather than dermal cells at this stage (Närhi et al., 2008). Primary hair follicle placodes are enlarged in *Sostd1l* null mice but do not display altered spacing, although patterning of certain other ectodermal appendages including mammary glands and vibrissae is altered (Närhi et al., 2012), and analyses of hair follicle patterning have not been described in mice lacking *Dkk1* or *Dkk4.* Thus, the possibility remains open that *Dkk2* contributes to placode patterning in hairy skin but performs functions that are redundant with those of other *Dkk* family members and/or *Sostdc1.*

Interestingly, our data revealed that the process of ectopic hair follicle formation in plantar skin of *Dkk2* mutants involves broad activation of Wnt/β-catenin signaling in the dermis and epidermis, followed by its gradual refinement to defined locations. These events mimic the gradual patterning of Wnt/β-catenin activity observed during normal hair follicle development in dorsal skin (Chen et al., 2012; Zhang et al., 2009), a process thought to require reaction-diffusion mechanisms that involve competition between Wnt ligands and secreted Wnt inhibitors (Sick et al., 2006). Thus, while DKK2 is necessary to dictate absence of hair follicles in plantar skin, it is not required for the patterning of either normal or ectopic follicles, which must therefore involve other inhibitory factors. These could include the related genes *Dkk1* and *Dkk4* that are specifically expressed in hair follicles after initiation of hair follicle development (Andl et al., 2002; Bazzi et al., 2007) and are activated in response to elevated Wnt/β-catenin signaling (Bazzi et al., 2007; Lieven et al., 2014). While we find that *Dkk1* and *Dkk4* are expressed at low levels in hairless wild-type plantar skin relative to their expression in wild-type hairy skin, their expression is likely induced in *Dkk2*$^{-/-}$ ectopic plantar placodes and could contribute to their patterning. In addition, we find that expression of *Sostdc1* localizes to plantar basal epidermis and ectopic hair follicles in *Dkk2*$^{-/-}$ mutants, suggesting its potential to limit Wnt signaling in the plantar region in the absence of *Dkk2.*

The data outlined here indicate that plantar skin retains all of the mechanisms needed to form hair follicles and that relief from DKK2-mediated Wnt inhibition is sufficient to initiate this process. Given evolutionary conservation of the roles of Wnt/β-catenin signaling in mammalian hair follicle biology (Marvin et al., 2011; Xu et al., 2017), it is likely that our findings are relevant to understanding how hairless skin forms in humans. It is also interesting to consider whether spatially restricted expression of Wnt inhibitors could contribute to other regional variations in hair follicle development that have long intrigued skin biologists. Examples include the formation of long, thick hairs in the human scalp, versus shorter thick hairs in the eyebrows and fine vellus hairs in many other body regions. The extreme rarity of hairy cutaneous malformations of human palms and soles complicates

analysis of their genetic origin; however, it is possible that such mutations bypass extracellular Wnt inhibitory mechanisms by activating signaling downstream of Wnt receptors.

It will be exciting in the future to probe whether similar Wnt inhibitory mechanisms operate to prevent formation of fully functional skin containing hair follicles in regenerative scenarios such as healing of severe burns and to determine whether small molecule Wnt inhibitor antagonists might be used to combat such mechanisms.

We find that in rabbit embryos, which, unlike mouse embryos, normally develop plantar hair, expression levels of *Dkk2* are similar in embryonic plantar and dorsal paw skin. Our data therefore suggest that evolutionary forces have altered expression of *Dkk2* in some species to allow hair development in plantar skin. While the mechanisms underlying this difference require further investigation, these could include mutation of *Dkk2* enhancer elements. In addition, the *Dkk2* gene is silenced via DNA hyper-methylation in several contexts (Mu et al., 2017; Zhu et al., 2012), and *Dkk2* mRNA is de-stabilized by multiple microRNAs (e.g., Hassan et al., 2012; Li et al., 2013; Lu et al., 2017). Thus, differential expression, activity, or targeting of chromatin modifying factors, altered expression of miRNAs, or evolutionary changes in miRNA target sites in the *Dkk2* 3'UTR could contribute to upregulation or repression of *Dkk2* mRNA levels in plantar skin of different species. Future studies examining species differences in the expression patterns of *Dkk2* and other secreted Wnt inhibitors are likely to shed additional light on the mechanisms by which specific hair follicle distributions and characteristics have evolved in mammals.

STAR⋆METHODS

CONTACT FOR REAGENT AND RESOURCE SHARING

Further information and requests for resources and reagents should be directed to and will be fulfilled by the Lead Contact, Sarah E. Millar (millars@pennmedicine.upenn.edu).

EXPERIMENTAL MODEL AND SUBJECT DETAILS

Mouse strains and genotyping—Mice *(Mus musculus)* were maintained on a mixed C57BL/6 / FVB/N / SJL background in a Specific Pathogen Free (SPF) barrier facility on a standard light-dark cycle. Cages were changed twice per week, and mice received water and chow *ad libitum.* A sentinel program was used to monitor animal health. Littermates of the same sex were randomly assigned to experimental groups. Mice were housed at no more than five per cage; males from different litters were not co-housed. *Dkk2* null (RRID:IMSR_JAX:030130), $Axin2^{LacZ}$ (RRID:IMSR_JAX:009120) and $Sostdc1^{lacZ}$ (RRID:MGI:4360517) mice have been described previously (Li et al., 2005; Lustig et al., 2002; Yanagita et al., 2006). *Dkk2* null mice were crossed to $Axin2^{lacZ}$ mice or $Sostdc1^{lacZ}$ mice for several generations to obtain $Dkk2^{-/-}$ $Axin2^{lacZ}$ mice, $Dkk2^{-/-}$ $Sostdc1^{lacZ}$ mice, and littermate control mice. Embryonic ages were determined from the time of appearance of a vaginal plug (E0.5). Male and female animals were analyzed at embryonic and neonatal stages, and no sex-related differences were observed. Male mice were used for analysis of postnatal hair growth, as the timing of hair follicle cycling is variable in female mice. Mice

were genotyped by PCR of tail biopsy DNA. Primer sequences are provided in Table S1. All animal experiments were conducted under protocols approved by the University of Pennsylvania IACUC Committee.

Rabbit tissue—Freshly harvested or 4% paraformaldehyde-fixed New Zealand White (NZW) rabbit embryo tissues were purchased from Covance Research Products, Denver, PA (Cat#NZ-CTM).

METHOD DETAILS

Histology and immunostaining—Tissues were fixed in 4% paraformaldehyde at 4°C overnight, paraffin embedded and sectioned at 5 mm for hematoxylin and eosin staining and immunofluorescence. For frozen sections, tissues were fixed in 4% paraformaldehyde at 4°C overnight, followed by overnight incubation at 4°C in 30% DEPC-treated sucrose, embedding in O.C.T. compound (ThermoFisher Scientific, Cambridge, MA, Cat#23–730-571), and cryosectioning at 8 mm. For immunofluorescence, sections were dehydrated, blocked with 5% goat serum, and then incubated in blocking reagent. Details of the antibodies used are provided in the Key Resources Table.

In situ* hybridization—In situ* hybridization probe templates were synthesized by PCR of E14.5 mouse cDNA, using primers containing T7 RNA polymerase binding sites to amplify *Dkk2* (GenBank: NM_020265.4, nt 1141–1970 or GenBank: NM_020265.4, nt 1125–1242) and *Ctnnb1* (GenBank: NM_007614, nt 150 – 540). Antisense digoxigenin-labeled RNA probes were prepared with MAXIscript T7 *in vitro* transcription kit (ThermoFisher Scientific, Cat#AN1312). The RNA probes were purified with MEGAclear Transcription Clean-Up Kit (ThermoFisher Scientific, Cat#AM1908) to remove free nucleotides.

For whole-mount RNA *in situ* hybridization, embryos were fixed in 4% paraformaldehyde overnight at 4°C and stored in methanol at −20°C. Rehydrated samples were treated with proteinase K and incubated with 1 μg digoxigenin-labeled RNA probe in 1 ml hybridization buffer at 70°C. After overnight incubation, embryos were washed in 2X saline sodium citrate buffer at 70°C and then treated with RNAase A solution (10 μg/ml) at 37°C to remove non-specific binding. After washing, embryos were incubated with anti-digoxigenin alkaline phosphatase in blocking buffer (Roche, Branchburg, NJ, DIG Nuclei Acid Detection Kit, Cat#11175041910) at 4°C overnight. After 72 hours of washing with 1X washing buffer (Roche, Cat#11175041910), embryos were incubated with detection buffer (Roche, Cat#11175041910) for 10 minutes. Signals were detected by immersing embryos in BM-Purple solution (Roche, Cat#11442074001) for 2–4 hours. After color development, tissues were fixed overnight in 4% paraformaldehyde, incubated in 30% sucrose, embedded in O.C.T and cryosectioned at 12 μm.

For RNA *in situ* hybridization with tissue sections, tissues were dissected in DEPC treated 1X PBS and fixed in 4% paraformaldehyde overnight. Fixed tissues were embedded in paraffin and sectioned at 6 μm. *In situ* hybridization assays were performed with antisense digoxigenin-labeled RNA probes. After overnight hybridization at 65°C, the slides were washed with 2X saline sodium citrate buffer and maleic acid buffer and incubated with anti-digoxigenin alkaline phosphatase (Roche, DIG Nuclei Acid Detection Kit,

Cat#11175041910) at 4°C overnight. The signals were developed with BCIP-NBT (Roche, DIG Nuclei Acid Detection Kit, Cat#11175041910).

Whole mounted embryos were photographed using a Leica MZ16F microscope and Leica DFC7000T digital camera (Leica Microsystems, Buffalo Grove, IL). Sections were photographed using a Leica DM5000B microscope and Leica digital cameras DFC 360 FX and DFC 420.

Alkaline Phosphatase Staining—Plantar skin was dissected and digested at 4°C overnight with 2 mg/ml Dispase II (ThermoFisher Scientific, Cat#17105041). Dermis was separated from epidermis using forceps, fixed in 4% paraformaldehyde at room temperature for 20 minutes, washed with DPBS (ThermoFisher Scientific, Cat#14190–136), rinsed once in AP buffer (100mM Tris-HCl, 5mM $MgCl_2$,100 mM NaCl, pH9.5), and incubated at 37°C for up to 4 hours in NBT/BCIP staining solution (Roche, Cat#11681451001). The reaction was stopped by rinsing with DPBS. Samples were photographed using a Leica MZ16F microscope and Leica DFC7000T digital camera (Leica Microsystems, Buffalo Grove, IL).

Scanning electron microscopy—Samples were fixed overnight in 4% PFA, dehydrated in graded ethanols, incubated for20 minutes in 50% HMDS in ethanol followed by three changes of 100% HMDS (Sigma-Aldrich, C7207, Cat#440911), air-dried overnight, mounted on stubs and sputter coated with gold palladium. Specimens were observed and photographed using a Quanta 250 scanning electron microscope (FEI, Hillsboro, OR) at 10 kV accelerating voltage.

Wax depilation—Sally Hansen Extra Strength Brazilian Bikini Wax (Amazon.com, Seattle, WA) was melted at 60°F in a Makartt Hair Removal Hot Wax Warmer (Amazon.com). *Dkk2*$^{-/-}$ mice were anesthetized with 1%−3% isofluorane using a nose cone prior to and during the procedure. Warm wax was applied and was peeled off after 3–5 minutes. Wax was re-applied after 10 minutes and peeling was repeated once to ensure removal of all ectopic plantar hair.

Quantitative PCR—Full thickness dorsal paw skin and plantar skin was dissected from mouse embryos at E18 and from rabbit embryos at E29. Full thickness plantar skin samples were dissected from *Dkk2*$^{+/-}$ and *Dkk2*$^{-/-}$ mouse pups at P0. Total RNA was extracted using RNeasy Plus Mini Kit (QIAGEN, Valencia, CA, Cat#74134) and cDNA synthesized using SuperScript III First-Strand Synthesis System (ThermoFisher Scientific, Cat#18080051). Reactions were set up using Fast SYBR Green Master Mix (ThermoFisher Scientific, Cat#4385612) following the manufacturer's instructions. The sequences of qPCR primers are provided in Table S1. Relative expression levels were calculated using the $2^{-\Delta\Delta CT}$ method and normalized to *Gapdh.* At least three biological replicates were assayed, and three technical replicates were performed for each sample. Statistical significance was calculated using two-tailed Student's t test.

X-gal staining—Whole mounted dissected mouse embryonic hind paws were fixed in 2% PFA for 1 hour on ice. After fixation, tissues were transferred to washing buffer containing 0.02% IGEPAL CA-630 (Sigma-Aldrich, Cat#18896), 0.01% sodium deoxycholate and

2mM $MgCl_2$ in 1x PBS for 3 hours and then incubated at 37°C for 5 hours in the dark in 1mg/ml X-gal (EMD Millipore, Cat#BG-3-G) in Base Solution (EMD Millipore, Cat#BG-8-C). After staining, tissues were fixed in 4% PFA, incubated in 30% sucrose, embedded in O.C.T and cryosectioned at 12 μm.

QUANTIFICATION AND STATISTICAL ANALYSIS

We utilized n = 5 control and n = 5 experimental mice wherever possible, providing 80% power at a two-sided significance level of 0.05 to detect a difference (effect size) of 2.0 s where s is the standard deviation; at a minimum we utilized n = 3 control and n = 3 experimental mice, providing 80% power at a two-sided significance level of 0.05 to detect a difference of 2.8 s. For quantitation of *rDkk2* levels, n = 5 plantar and n = 5 dorsal paw skin samples from rabbit embryos were analyzed. Statistical significance was calculated using Student's t test. Statistical parameters are reported in the relevant Figure Legends.

Supplementary Material

Refer to Web version on PubMed Central for supplementary material.

ACKNOWLEDGMENTS

We thank Xiaoling Zhang for statistical analysis support and Donna Brennan-Crispi for X-gal staining protocols. This work was supported by a scholarship from China Scholarship Council, China (to Y.S.); National Institutes of Health (NIH), USA (R37AR047709 to S.E.M.); NIH, USA (Penn Skin Diseases Research Center P30AR057217); NIH, USA (Penn Skin Biology and Diseases Resource-based Center P30AR069589); and a Career Development Award from the Dermatology Foundation, USA (to M.X.). G.G.L. works under the auspices of the United States Department of Energy, USA (DE-AC52–07NA27344) at Lawrence Livermore National Laboratory.

REFERENCES

Ahn Y, Sanderson BW, Klein OD, and Krumlauf R (2010). Inhibition of Wnt signaling by Wise (Sostdc1) and negative feedback from Shh controls tooth number and patterning. Development 137, 3221–3231. [PubMed: 20724449]

Andl T, Reddy ST, Gaddapara T, and Millar SE (2002). WNT signals are required for the initiation of hair follicle development. Dev. Cell 2, 643–653. [PubMed: 12015971]

Bafico A, Liu G, Yaniv A, Gazit A, and Aaronson SA (2001). Novel mechanism of Wnt signalling inhibition mediated by Dickkopf-1 interaction with LRP6/Arrow. Nat. Cell Biol. 3, 683–686. [PubMed: 11433302]

Bazzi H, Fantauzzo KA, Richardson GD, Jahoda CA, and Christiano AM (2007). The Wnt inhibitor, Dickkopf 4, is induced by canonical Wnt signaling during ectodermal appendage morphogenesis. Dev. Biol. 305, 498–507. [PubMed: 17397822]

Chen D, Jarrell A, Guo C, Lang R, and Atit R (2012). Dermal p-catenin activity in response to epidermal Wnt ligands is required for fibroblast proliferation and hair follicle initiation. Development 139, 1522–1533. [PubMed: 22434869]

Clevers H, and Nusse R (2012). Wnt/β-catenin signaling and disease. Cell 149, 1192–1205. [PubMed: 22682243]

Cui CY, Yin M, Sima J, Childress V, Michel M, Piao Y, and Schles- singer D (2014). Involvement of Wnt, Eda and Shh at defined stages of sweat gland development. Development 141, 3752–3760. [PubMed: 25249463]

Gage PJ, Qian M, Wu D, and Rosenberg KI (2008). The canonical Wnt signaling antagonist DKK2 is an essential effector of PITX2 function during normal eye development. Dev. Biol. 317, 310–324. [PubMed: 18367164]

Hassan MQ, Maeda Y, Taipaleenmaki H, Zhang W, Jafferji M, Gordon JA, Li Z, Croce CM, van Wijnen AJ, Stein JL, et al. (2012). miR-218 directs a Wnt signaling circuit to promote differentiation of osteoblasts and osteomimicry of metastatic cancer cells. J. Biol. Chem. 287 42084–42092. [PubMed: 23060446]

Huber O, Korn R, McLaughlin J, Ohsugi M, Herrmann BG, and Kemler R (1996). Nuclear localization of beta-catenin by interaction with transcription factor LEF-1. Mech. Dev. 59, 3–10. [PubMed: 8892228]

Huelsken J, Vogel R, Erdmann B, Cotsarelis G, and Birchmeier W (2001). beta-Catenin controls hair follicle morphogenesis and stem cell differentiation in the skin. Cell 105, 533–545. [PubMed: 11371349]

Jackson CE, Callies QC, Krull EA, and Mehregan A (1975). Hairy cutaneous malformations of palms and soles. A hereditary condition. Arch. Dermatol. 111, 1146–1149. [PubMed: 810092]

Kamberov YG, Karlsson EK, Kamberova GL, Lieberman DE, Sabeti PC, Morgan BA, and Tabin CJ (2015). A genetic basis of variation in eccrine sweat gland and hair follicle density. Proc. Natl. Acad. Sci. USA 112, 9932–9937. [PubMed: 26195765]

Li X, Liu P, Liu W, Maye P, Zhang J, Zhang Y, Hurley M, Guo C, Bos-key A, Sun L, et al. (2005). Dkk2 has a role in terminal osteoblast differentiation and mineralized matrix formation. Nat. Genet. 37, 945–952. [PubMed: 16056226]

Li X, Shan J, Chang W, Kim I, Bao J, Lee HJ, Zhang X, Samuel VT, Shulman GI, Liu D, et al. (2012). Chemical and genetic evidence for the involvement of Wnt antagonist Dickkopf2 in regulation of glucose metabolism. Proc. Natl. Acad. Sci. USA 109, 11402–11407. [PubMed: 22733757]

Li Q, Shen K, Zhao Y, He X, Ma C, Wang L, Wang B, Liu J, and Ma J (2013). MicroRNA-222 promotes tumorigenesis via targeting DKK2 and activating the Wnt/β-catenin signaling pathway. FEBS Lett. 587, 1742–1748. [PubMed: 23587485]

Lieven O, Dronka J, Burmuhl S, and Ruther U (2014). Differential binding of Lef1 and Msx1/2 transcription factors to Dkk1 CNEs correlates with reporter gene expression in vivo. PLoS ONE 9, e115442. [PubMed: 25545010]

Lintern KB, Guidato S, Rowe A, Saldanha JW, and Itasaki N (2009). Characterization of wise protein and its molecular mechanism to interact with both Wnt and BMP signals. J. Biol. Chem. 284, 23159–23168. [PubMed: 19553665]

Liu BY, McDermott SP, Khwaja SS, and Alexander CM (2004). The transforming activity of Wnt effectors correlates with their ability to induce the accumulation of mammary progenitor cells. Proc. Natl. Acad. Sci. USA 101, 4158–4163. [PubMed: 15020770]

Lu CP, Polak L, Keyes BE, and Fuchs E (2016). Spatiotemporal antagonism in mesenchymal-epithelial signaling in sweat versus hair fate decision. Science 354, aah6102.

Lu J, Wei JH, Feng ZH, Chen ZH, Wang YQ, Huang Y, Fang Y, Liang YP, Cen JJ, Pan YH, et al. (2017). miR-106b-5p promotes renal cell carcinoma aggressiveness and stem-cell-like phenotype by activating Wnt/β-catenin signalling. Oncotarget 8, 21461–21471. [PubMed: 28423523]

Lustig B, Jerchow B, Sachs M, Weiler S, Pietsch T, Karsten U, van de Wetering M, Clevers H, Schlag PM, Birchmeier W, and Behrens J (2002). Negative feedback loop of Wnt signaling through upregulation of con- ductin/axin2 in colorectal and liver tumors. Mol. Cell. Biol. 22, 1184–1193. [PubMed: 11809809]

Marvin ML, Mazzoni SM, Herron CM, Edwards S, Gruber SB, and Petty EM (2011). AXIN2-associated autosomal dominant ectodermal dysplasia and neoplastic syndrome. Am. J. Med. Genet. A 155A, 898–902. [PubMed: 21416598]

Mehregan AH, and Coskey RJ (1972). Pigmented nevi of sole. A report of two cases with histologic evidence of hair follicle formation. Arch. Dermatol. 106, 886–887. [PubMed: 4639252]

Millar SE (2002). Molecular mechanisms regulating hairfollicle development. J. Invest. Dermatol. 118, 216–225. [PubMed: 11841536]

Morris RJ, Liu Y, Marles L, Yang Z, Trempus C, Li S, Lin JS, Sawicki JA, and Cotsarelis G (2004). Capturing and profiling adult hair follicle stem cells. Nat. Biotechnol. 22, 411–417. [PubMed: 15024388]

Mu J, Hui T, Shao B, Li L, Du Z, Lu L, Ye L, Li S, Li Q, Xiao Q, et al. (2017). Dickkopf-related protein 2 induces G0/G1 arrest and apoptosis through suppressing Wnt/β-catenin signaling and is frequently methylated in breast cancer. Oncotarget 8, 39443–39459. [PubMed: 28467796]

Mukhopadhyay M, Gorivodsky M, Shtrom S, Grinberg A, Niehrs C, Mo- rasso MI, and Westphal H (2006). Dkk2 plays an essential role in the corneal fate of the ocular surface epithelium. Development 133, 2149–2154. [PubMed: 16672341]

Närhi K, Jarvinen E, Birchmeier W, Taketo MM, Mikkola ML, and The-sleff I (2008). Sustained epithelial beta-catenin activity induces precocious hair development but disrupts hair follicle down-growth and hair shaft formation. Development 135, 1019–1028. [PubMed: 18256193]

Närhi K, Tummers M, Ahtiainen L, Itoh N, Thesleff I, and Mikkola ML (2012). Sostdc1 defines the size and number of skin appendage placodes. Dev. Biol. 364, 149–161. [PubMed: 22509524]

Niehrs C (2006). Function and biological roles of the Dickkopf family of Wnt modulators. Oncogene 25, 7469–7481. [PubMed: 17143291]

Plikus M, and Chuong CM (2004). Making waves with hairs. J. Invest. Dermatol. 122, vii–ix.

Schnitzler ML (1973). Dysembryoplasie pilaire circonscrite des paumes: un cas familial. Bull. Soc. Franc. Derm. Syph. 80, 323–324.

Semenov MV, Tamai K, Brott BK, Kühl M, Sokol S, and He X (2001). Head inducer Dickkopf-1 is a ligand for Wnt coreceptor LRP6. Curr. Biol. 11, 951–961. [PubMed: 11448771]

Sick S, Reinker S, Timmer J, and Schlake T (2006). WNT and DKK determine hair follicle spacing through a reaction-diffusion mechanism. Science 314, 1447–1450. [PubMed: 17082421]

Vidal VP, Chaboissier MC, Lützkendorf S, Cotsarelis G, Mill P, Hui CC, Ortonne N, Ortonne JP, and Schedl A (2005). Sox9 is essential for outer root sheath differentiation and the formation of the hair stem cell compartment. Curr. Biol. 15, 1340–1351. [PubMed: 16085486]

Xu M, Horrell J, Snitow M, Cui J, Gochnauer H, Syrett CM, Kallish S, Seykora JT, Liu F, Gaillard D, et al. (2017). WNT10A mutation causes ectodermal dysplasia by impairing progenitorcell proliferation and KLF4-mediated differentiation. Nat. Commun. 8, 15397. [PubMed: 28589954]

Yanagita M, Okuda T, Endo S, Tanaka M, Takahashi K, Sugiyama F, Kunita S, Takahashi S, Fukatsu A, Yanagisawa M, et al. (2006). Uterine sensitization-associated gene-1 (USAG-1), a novel BMP antagonist expressed in the kidney, accelerates tubular injury. J. Clin. Invest. 116, 70–79. [PubMed: 16341262]

Zhang Y, Andl T, Yang SH, Teta M, Liu F, Seykora JT, Tobias JW, Piccolo S, Schmidt-Ullrich R, Nagy A, et al. (2008). Activation of beta-catenin signaling programs embryonic epidermis to hair follicle fate. Development 135, 2161–2172. [PubMed: 18480165]

Zhang Y, Tomann P, Andl T, Gallant NM, Huelsken J, Jerchow B, Birchmeier W, Paus R, Piccolo S, Mikkola ML, et al. (2009). Reciprocal requirements for EDA/EDAR/NF-kappaB and Wnt/beta-catenin signaling pathways in hair follicle induction. Dev. Cell 17, 49–61. [PubMed: 19619491]

Zhou P, Byrne C, Jacobs J, and Fuchs E (1995). Lymphoid enhancer factor 1 directs hair follicle patterning and epithelial cell fate. Genes Dev. 9, 700–713. [PubMed: 7537238]

Zhu J, Zhang S, Gu L, and Di W (2012). Epigenetic silencing of DKK2 and Wnt signal pathway components in human ovarian carcinoma. Carcinogenesis 33, 2334–2343. [PubMed: 22964660]

Highlights

- DKK2 localizes to embryonic mouse hairless, but not rabbit hairy, plantar skin
- Deletion of mouse *Dkk2* causes formation of mature, regenerative plantar hair
- *Dkk2* specifies development of hairless versus hairy skin
- Evolutionary changes in Dkk2 regulation underlie speciesspecific hair patterns

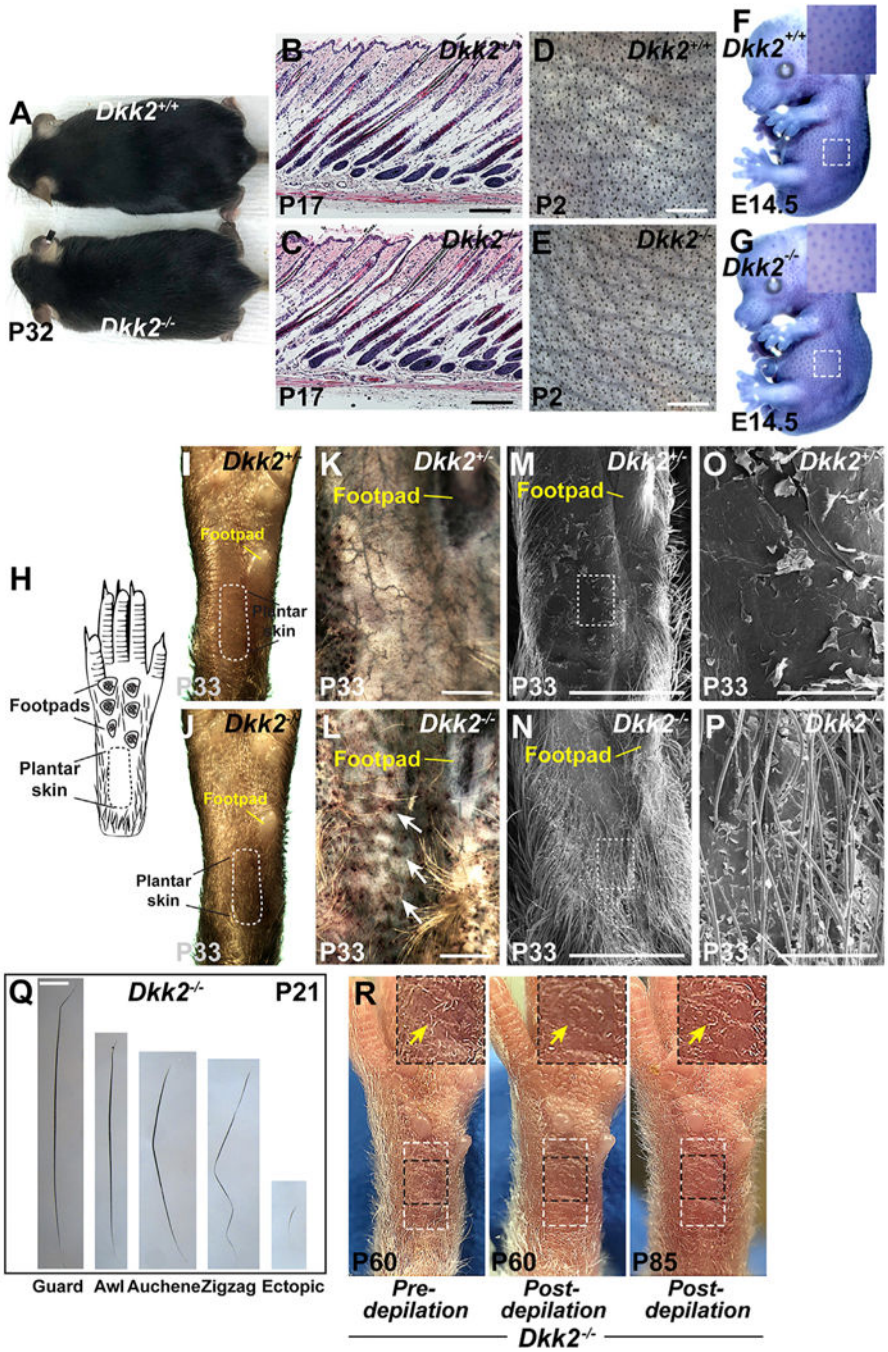

Figure 1. Ectopic Hair Follicles Form In Plantar Skin of *Dkk2* Null Mice.

(A)Normal appearance of the hair coat of *Dkk2*$^{-/-}$ mouse at P32 compared with a wild-type littermate control (n > 40 mutants and littermate controls). (B and C) Indistinguishable histology of *Dkk2*$^{-/-}$ (C) and *Dkk2*$^{+/+}$control littermate (B) dorsal skin at P17 (n = 3 mutants and n = 3 littermate controls). (D and E) Light microscopy of dissected dorsal skin at P2 reveals similar density and patterning of primary and secondary hair follicles in Dkk2$^{-/-}$ (E) and *Dkk2*$^{+/+}$ control (D) littermate mice (n = 3 mutants and n = 3 littermate controls). (F and G) Whole mount *in situ* hybridization for *Ctnnb1* (purple-blue signal)

reveals similar sizes and patterning of primary hair follicle placodes in Dkk2$^{-/-}$ (G) and Dkk2$^{+/+}$control (F) littermate embryos at E14.5 (n = 3 mutants and n = 3 littermate controls). Insets: higher magnification views of the boxed areas. (H) Schematic indicating the locations of footpads and plantar skin on the ventral side of a right hind foot. A dashed black line marks the border of plantar skin. (I-P) Light microscopy (I and J), alkaline phosphatase staining (purple/brown) of dissected plantar dermis (K and L), and scanning EM micrographs (M-P) of the ventral side of right hind feet from *Dkk2*$^{+/-}$control (I, K, M, and O) and *Dkk2*$^{-/-}$ (J, L, N, and P) mice at P33 (n > 40 mutants and n > 40 controls for I and J; n = 3 mutants and n = 3 littermate controls for each experiment in K-P). The plantar region is delineated by a dashed white line in (I) and (J). White arrows in (L) indicate ectopic alkaline phosphatase-positive hair follicle dermal papillae. (O) and (P) are higher magnification views of the boxed regions in (M) and (N), respectively. Locations of the footpads are indicated in (I)-(N). Note formation of fully formed ectopic hair in *Dkk2*$^{-/-}$ plantar skin. (Q) Morphology of ectopic hair shaft compared with normal guard, awl, auchene, and zigzag hairs plucked from ventral limb skin at P21. Ectopic hair is shorter and finer than normal hair (n = 3 mutant mice analyzed). (R) Photographs of right hind foot of a *Dkk2*$^{-/-}$ mouse prior to depilation of the plantar region at P60 (left), immediately following depilation (middle), and 25 days later (P85) (right). Areas outlined with a dashed white box indicate the plantar region. Insets: higher magnification views of areas outlined by dashed black boxes. Arrows indicate ectopic plantar hair (left); lack of hair after depilation (middle); and re-growth of ectopic hair at P85 (right) (n = 3 *Dkk2*$^{-/-}$ mice depilated). Scale bars, 150 μm (B and C); 1.5 mm (D and E); 359 μm (K and L); 2 mm (M and N); 300 μm (O and P); 700 μm (Q). See also Figure S1.

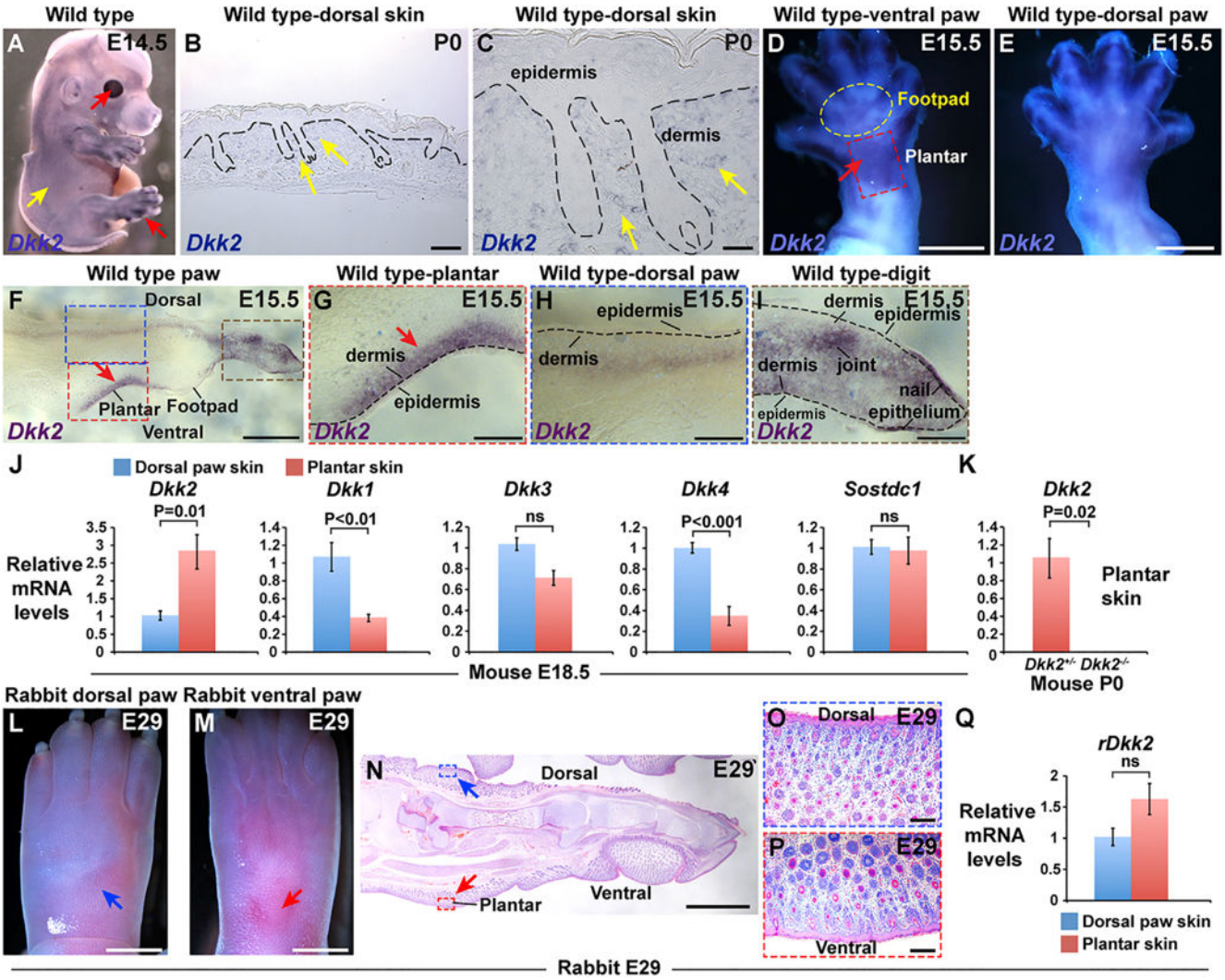

Figure 2. *Dkk2* Is Specifically Upregulated In Plantar Dermis of Mouse but Not Rabbit Embryos.

(A) Whole mount *in situ* hybridization for *Dkk2* in wild-type mouse embryo at E14.5 (purple signal) reveals high expression levels in cornea and digits (red arrows) and low levels of expression in trunk and head skin between, but not within, hair follicle placodes (yellow arrow) (n = 6 biological replicates). (B) *In situ* hybridization for *Dkk2* in sectioned wild-type mouse P0 dorsal skin (dark blue signal). (C) Higher magnification view of the area indicated by arrows in (B). Note low level expression in inter-follicular dermis (yellow arrows) (n = 3 biological replicates in B and C). (D and E) Ventral (D) and dorsal (E) views of an E15.5 mouse hind limb subjected to whole mount *in situ* hybridization for *Dkk2* (purple-blue signal). Note high expression in the plantar region of the mouse ventral hind limb at E15.5 (arrow in D) (n = 4). (F) Cryosectioned mouse E15.5 hind limb following whole mount *in situ* hybridization for *Dkk2* (purple signal) (n = 5 biological replicates). (G-I) higher magnification views of areas of (F) outlined with a dashed red box (G), a dashed blue box (H), and a dashed brown box (I). Note specific expression of *Dkk2* in plantar dermis (arrows in F and G) compared with adjacent footpad skin and dorsal limb dermis at E15.5; low to undetectable levels of *Dkk2* in dorsal limb dermis (H); and stronger signal in tissue located

at a deeper level in the limb (H). In the limb digit, *Dkk2* expression localizes to ventral but not dorsal dermis; relatively high levels of *Dkk2* expression are also observed in nail epithelium and in the developing joint region (I). Dashed black lines in (B), (C), and (G)-(I) represent the dermal-epidermal border. (J) Relative levels of *Dkk2, Dkk1, Dkk3, Dkk4,* and *Sostdc1* mRNA in full thickness dorsal paw skin (blue boxes) and plantar skin (pink boxes) from E18.5 mouse embryos, analyzed by qPCR (n = 5 plantar skin samples and n = 5 dorsal paw skin samples in each experiment). Note that only *Dkk2* is specifically enriched in plantar skin. (K) Relative levels of *Dkk2* mRNA in full thickness mouse $Dkk2^{+/-}$ control (pink box) and $Dkk2^{-/-}$mutant (black box) plantar skin at P0, analyzed by qPCR (n = 3 littermate controls and n = 3 mutants). *Dkk2* transcript levels are undetectable in $Dkk2^{-/-}$ skin. (L and M) Light microscopy of dorsal (L) and ventral (M) left hind paw of a rabbit embryo at E29. Developing hair follicles are present in the ventral plantar region (red arrow, M), as well as in dorsal skin (blue arrow, L). (N) Histology of embryonic rabbit left hind paw at E29 showing the presence of developing hair follicles in ventral plantar skin (red arrow) as well as dorsal paw skin (blue arrow). (O and P) Higher magnification views of the areas indicated in (N) by blue (O) and red (P) dashed boxes, respectively (5 biological replicates for L-P). (Q) Relative levels of *rDkk2* mRNA in full thickness dorsal paw skin (blue box) and plantar skin (pink box)from E29 rabbit embryos, analyzed by qPCR (n = 5 plantar skin samples and n = 5 dorsal paw skin samples). Levels of *rDkk2* mRNA are not significantly different between embryonic rabbit dorsal and plantar paw skin. All qPCR assays were performed in triplicate for each sample and data were normalized to *Gapdh;* mean values ± SD are shown. Statistical significance was calculated using Student's t test. Scale bars, 100 μm (B); 30 μm (C); 750 μm (D and E); 470 μm (F); 150 μm (G-I, O, and P); 3 mm (L and M); 2 mm (N). See also Figure S2.

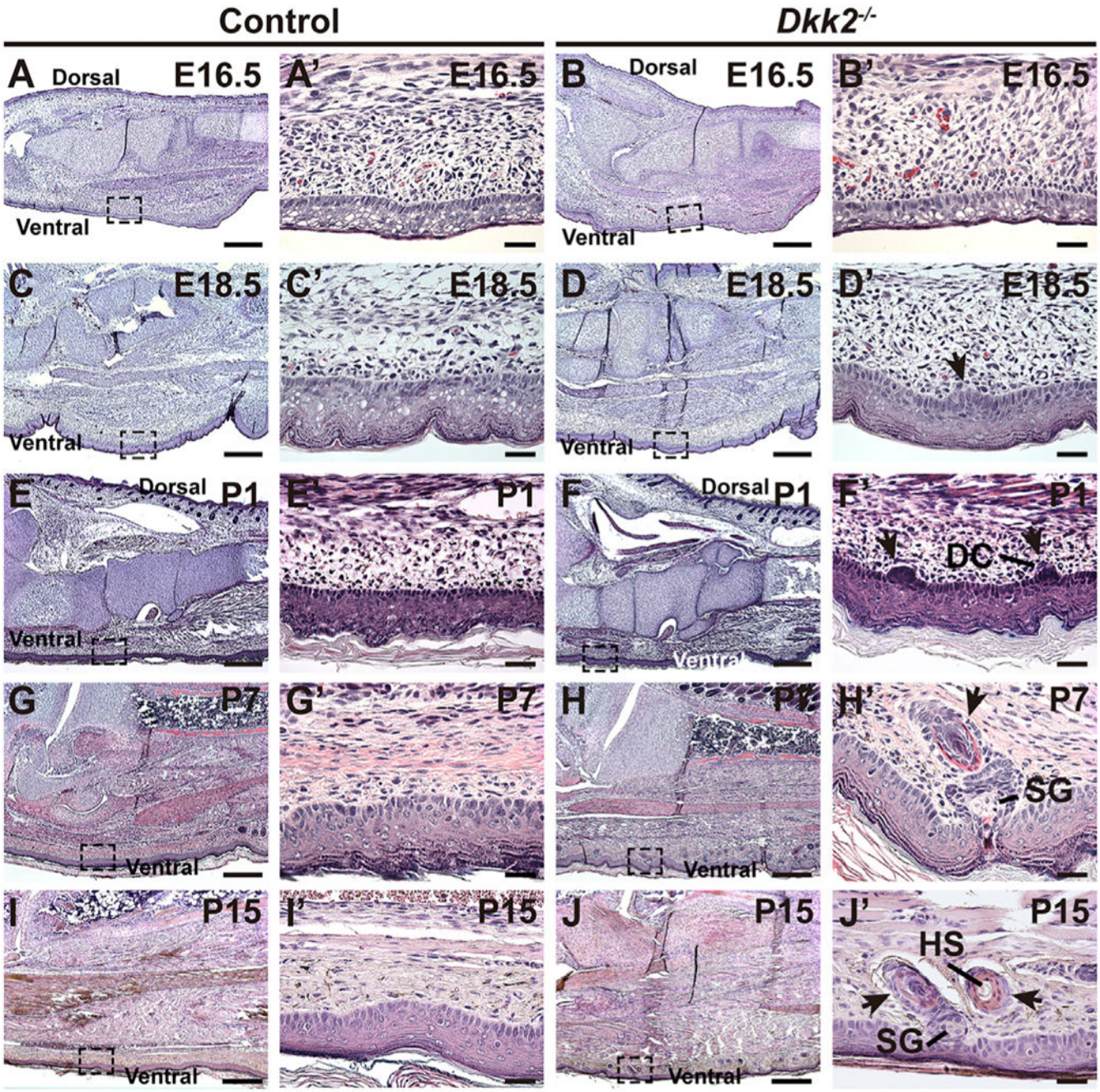

Figure 3. Ectopic Hair Follicle Placodes Form in *Dkk2*$^{-/-}$ Plantar Skin by E18.5 and Mature Postnatally.

(A-J′) Histology of hind foot skin from control littermate and *Dkk2*$^{-/-}$ mice as indicated, at E16.5 (A-B′), E18.5 (C-D′), P1 (E-F′), P7 (G-H′), and P15 (I-J′). Ectopic placodes are present in *Dkk2*$^{-/-}$ plantar skin by E18.5 (D′, arrow), form hair germs by P1 (F′, arrows), and display differentiated structures at P7 and P15 (H′and J′, arrows). Boxed areas of ventral skin in (A)-(J) are shown at higher magnification in (A′)-(J′). Control genotypes were *Dkk2*$^{+/-}$ (A, A′, E, and E′) or *Dkk2*$^{+/+}$ (C, C′, G, G′, I, and I′). n = 3 mutants and n = 3 littermate controls for each

analysis. DC, dermal condensate; SG, sebaceous gland; HS, hair shaft. Scale bars, 300 mm (A-J); 30 mm (A′-J′). See also Figure S3.

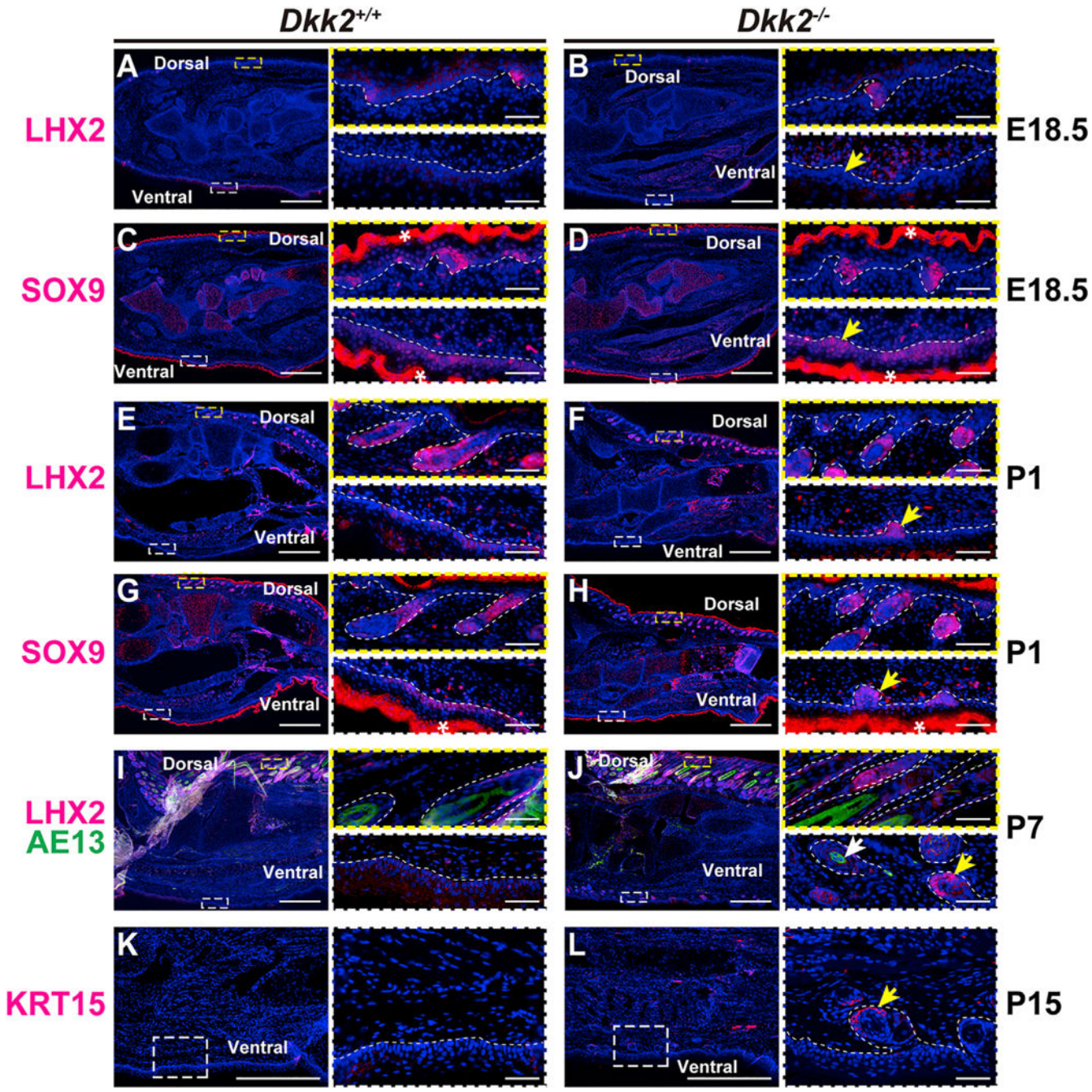

Figure 4. Ectopic Hair Follicles Express the Same Differentiation and Stem Cell Markers as Normal Hair Follicles.

(A-L) Immunofluorescence staining of littermate *Dkk2*$^{+/+}$ control (A, C, E, G, I, and K) and *Dkk2*$^{-/-}$ mutant (B, D, F, H, J, and L) sectioned mouse hind paws at E18.5 (A-D), P1 (E-H), P7 (I and J), and P15 (K and L) using antibodies to the hair follicle marker LHX2 (A, B, E, F, I, and J) (red), the outer root sheath and stem cell marker SOX9 (C, D, G, and H) (red), the hair shaft differentiation marker AE13 (I and J) (green), and the bulge stem cell marker KRT15 (K and L) (red). Dorsal skin regions outlined by dashed yellow boxes in (A)-(L) are shown at higher magnification to the upper right of each panel. Plantar skin regions outlined

by dashed white boxes in (A)-(L) are shown at higher magnification to the lower right of each panel. n = 3 mutants and n = 3 littermate controls for each analysis. Ectopic plantar structures express the hair follicle marker SOX9 from E18.5 (D and H), and LHX2 from P1 (F and J) (yellow arrows), indicating they are hair follicles rather than sweat glands, which do not express LHX2. Expression of AE13 indicates production of keratinized hair shaft structures in ectopic follicles (J) (white arrow), and expression of KRT15 indicates that the ectopic follicles contain a bulge stem cell population (L) (yellow arrow). These markers are expressed in dorsal but not plantar skin of wild-type controls (A, C, E, G, I, and K). Dashed white lines indicate epidermal/dermal borders. Nuclei were counterstained with DAPI (blue). 'Non-specific fluorescence. Scale bars, 500 μm (low-magnification images) and 50 μm (boxed areas photographed at higher magnification).

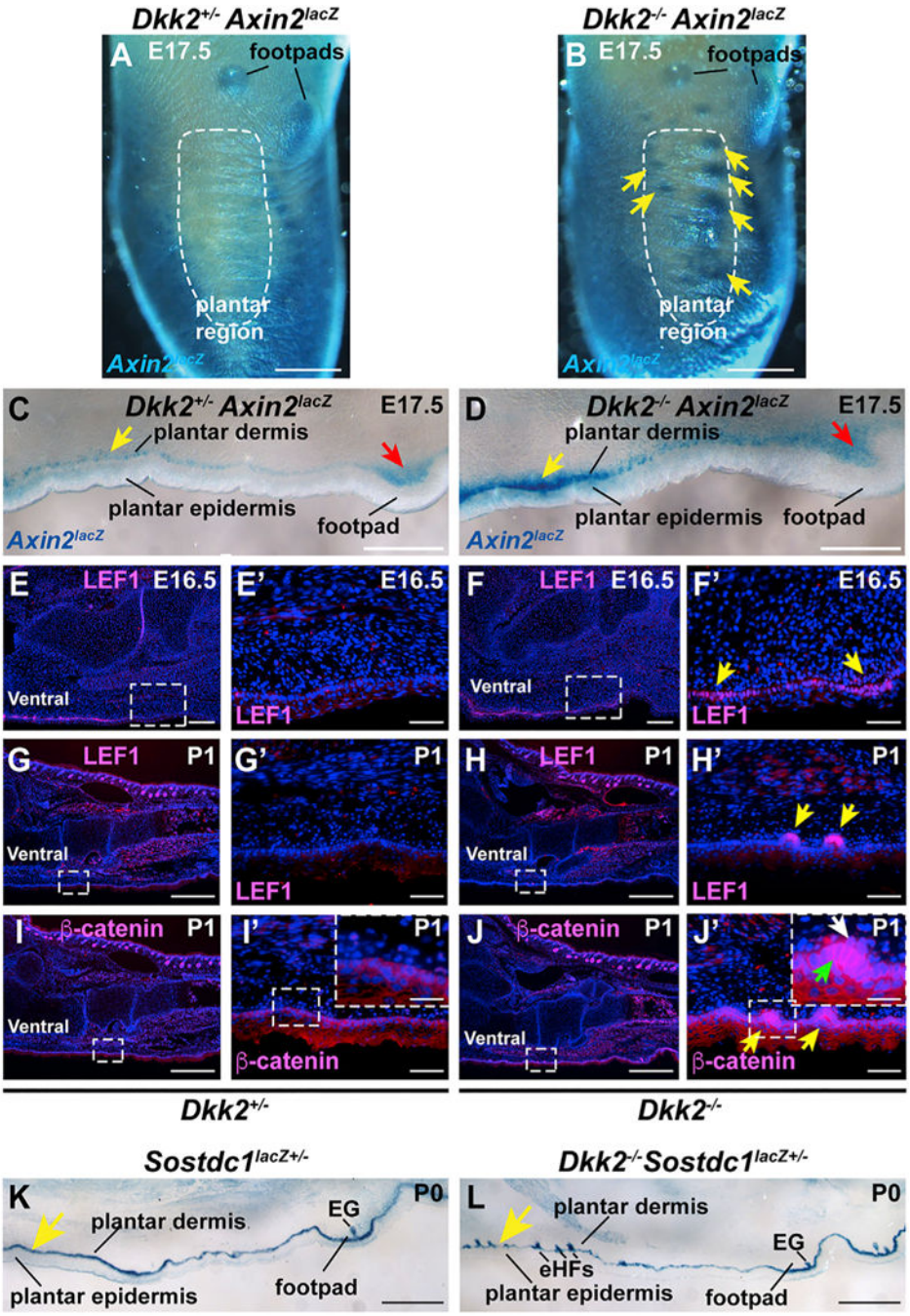

Figure 5. Wnt/β-Catenin Signaling Is Elevated in Embryonic and Neonatal *Dkk2*$^{-/-}$ Plantar Skin.

(A and B) X-gal-stained whole mounted control *Dkk2*$^{+/-}$ *Axin2*^{lacZ} (A) and *Dkk2*$^{-/-}$ *Axin2*^{laaZ} (B) hind paws at E17.5. Note elevated *Axin2*^{lacZ} Wnt reporter activity (blue signal) in the developing plantar region of the *Dkk2*$^{-/-}$ mutant (B, arrows). The plantar region is outlined by a dashed white line in (A) and (B) and footpad locations are indicated. (C and D) Cryosections of ventral skin from X-gal stained *Dkk2*$^{+/-}$ *Axin2*^{lacZ}control littermate (C) and Dkk2$^{-/-}$ *Axin2*^{lacZ} (D) hind paw whole mounts at E17.5. Wnt reporter expression is elevated in plantar papillary dermis and plantar epidermis in the Dkk2$^{-/-}$

mutant compared with the control (yellow arrows). Signaling levels are similar in mutant and control footpads (red arrows). (E-J′) Hind paw sections from *Dkk2*$^{+/-}$ control littermate (E, E′, G, G′, I, and I′) and *Dkk2*$^{-/-}$ (F, F′, H, H′, J, and J′) mice at E16.5 (E-F′) or P1 (G-J′) subjected to immunofluorescence (pink signal) for LEF1 (E-H′) or p-catenin (I-J′). Boxed areas in (E)-(J) are shown at higher magnification in (E′)-(J′). Boxed areas in (I′) and (J′) are shown at further increased magnification in the insets. Yellow arrows indicate ectopic expression of LEF1 or β-catenin in Dkk2$^{-/-}$ plantar skin. Green arrow in (J′) inset indicates nuclear and cytoplasmic localization of β-catenin in epithelial cells and white arrow in (J′) inset indicates nuclear localized β-catenin in the dermal condensate of an ectopic hair germ. (K and L) Expression of the Wnt inhibitor *Sostdc1* in cryosectioned X-gal stained littermate control (K) and Dkk2$^{-/-}$ mutant (L) ventral paw skin at P1, indicated by expression of a lacZ reporter (blue staining) knocked into the *Sostdc1* locus. Note expression of *Sostdc1* in plantar and footpad basal epidermis in both control and littermate samples; *Sostdc1* also localizes to sweat glands in the footpad of both control and mutant and to ectopic hair follicles in the mutant plantar region. n = 3 mutants and n = 3 littermate controls for each analysis in (A)-(L). EG, eccrine gland; eHFs, ectopic hair follicles. Scale bars, 500 μm (A and B); 300 μm (C and D); 500 μm (E-J); 50 μm (E′-J′); 20 μm (insets in I′and J′); 400 μm (K and L).

KEY RESOURCES TABLE

REAGENT or RESOURCE	SOURCE	IDENTIFIER
Antibodies		
Rabbit monoclonal anti-Ki67 (1:200)	Abcam	Cat#ab16667; RRID AB_302459
Rabbit monoclonal anti-LEF1 (1:100)	Cell Signaling	Cat#2286s; RRID AB_10706166
Mouse monoclonal anti-b-catenin (1:1000)	Sigma-Aldrich	Cat# C7207; RRID AB_476865
Rabbit polyclonal anti-LHX2 (1:200)	Millipore	Cat# ABE1402; RRID AB_2722523
Rabbit polyclonal anti-Keratin10 (1:1000)	Covance	Cat# PRB-159P; RRID AB_291580
Rabbit polyclonal anti-Keratin14 (1:1000)	BioLegend	Cat#905301; RRID AB_2565048
Rabbit polyclonal anti-Loricrin (1:1000)	BioLegend	Cat# PRB-145P; RRID AB_10064155
Rabbit polyclonal anti-Involucrin (1:1000)	BioLegend	Cat# PRB-140C; RRID AB_291569
Rabbit polyclonal anti-SOX9 (1:200)	EMD-Millipore	Cat#AB5535, RRID:AB_2239761
Mouse monoclonal anti-hair cortex keratin (AE13) (1:100)	Abcam	Cat#ab16113, RRID:AB_302268
Mouse monoclonal anti-Keratin15 (1:2000)	Abnova Corporation	Cat#MAB10723, RRID:AB_11189389
Goat anti-Mouse IgG, Alexa Fluor 555 (1:1000)	ThermoFisher	Cat# A21425; RRID AB_1500751
Goat anti-Rabbit IgG, Alexa Fluor 555 (1:1000)	ThermoFisher	Cat# A21428; RRID AB_141784
Critical Commercial Assays		
RNeasy Fibrous Tissue Mini Kit	QIAGEN	Cat#74704
SuperScript III First-Strand Synthesis System	ThermoFisher	Cat#18080–051
Fast SYBR Green Master Mix	ThermoFisher	Cat#4385612
Experimental Models: Organisms/Strains		
Mouse: *Dkk2*^{tm1Dwu}, mixed C57BL/6 / FVB/N / SJL strain background	The Jackson Laboratory	RRID:IMSR_JAX:030130
Mouse: *Axin2*^{tm1Wbm}, mixed C57BL/6 / FVB/N / SJL strain background	The Jackson Laboratory	RRID:IMSR_JAX:009120
Mouse: *Sostdc1*^{lacZ}, mixed C57BL/6 / FVB/N / SJL strain background	Dr. Gabriela Loots, Lawrence Livermore National Laboratory	RRID:MGI:4360517
Rabbit: New Zealand white (NZW)	Covance Research Products	NZ-CTM
Oligonucleotides		
Please see Table S1	N/A	N/A
Recombinant DNA		
In situ hybridization probe for *Dkk2* GenBank: NM_020265.4 nt 1141–1970	This paper	N/A
In situ hybridization probe for *Dkk2* GenBank: NM_020265.4, nt 1125–1242	This paper	N/A
In situ hybridization probe for *Ctnnb1* (β-catenin) GenBank: NM 007614, nt 150–540	Zhang et al., 2009	N/A